REVIEW

Conjugated D–A terpolymers for organic field-effect transistors and solar cells

Hewei Luo[1], Zitong Liu[2] and Deqing Zhang[2]

The incorporation of additional electron donors or acceptors into the backbones of conjugated polymers with alternating donors and acceptors results in various conjugated D–A terpolymers. The presence of additional electron donors or acceptors in the conjugated backbones can modulate the electronic absorptions and highest occupied molecular orbital/lowest unoccupied molecular orbital levels, as well as interchain interactions and thin-film morphology. Because of these structural features, conjugated D–A terpolymers have been intensively investigated in recent years for applications in field-effect transistors and photovoltaic cells. In this review, we introduce the recent developments of conjugated D–A terpolymers with various combinations of electron donors and acceptors, and discuss the future perspectives for conjugated terpolymers.

In recent decades, conjugated polymers have demonstrated promising applications in flexible, large-area and low-cost electronic devices, such as organic field-effect transistors (OFETs)[1–3] and solar cells (OSCs).[4–7] This is attributed to the conjugated electronic and polymeric structures of these polymers, resulting in semiconducting properties with good solution processability, mechanical property and thermal stability.[8,9] Among the conjugated polymers, conjugated alternating polymers consisting of both electron donors (D) and electron acceptors (A), referred to as conjugated D–A polymers,[10–17] have been extensively investigated in recent years. The studies indicate that electronic absorptions, highest occupied molecular orbital/lowest unoccupied molecular orbital (HOMO/LUMO) energies (and bandgaps), interchain interactions and thin-film morphologies of conjugated D–A polymers can be effectively tuned[10–17] by properly varying the electron donors and acceptors as well as the linkers. Consequently, the semiconducting performance of conjugated D–A polymers can be tuned in this way. In fact, polymeric p-type, n-type and even ambipolar semiconductors with high charge mobilities have been developed on the basis of conjugated D–A polymers.[18–21] Moreover, conjugated D–A polymers have been successfully utilized as either electron donors or acceptors for OSCs with high power conversion efficiencies (PCEs).[22–25]

Apart from conjugated polymers with alternating electron donor and acceptor moieties, conjugated D–A terpolymers, which contain either one kind of acceptor/two types of electron donors (2D1A) or one kind of donor/two types of electron acceptors (1D2A) in the backbones as illustrated in Scheme 1, have received increased attention. It is expected that an additional dimension is generated for tuning the electronic structures of conjugated polymers and thus their absorptions and HOMO/LUMO levels as well as interchain packing[8,26] with such conjugated D–A terpolymers. Moreover, the combination of existing electron donors and acceptors can yield a huge number of terpolymers, which can be prepared in the same manner as conventional D–A polymers with alternating donor and acceptor moieties via Stille or Suzuki coupling reactions. A number of terpolymers have been reported, which show comparable and even superior semiconducting and photovoltaic performance in comparison with normal conjugated D–A polymers.

In this review, we mainly discuss the recent developments since 2013 for conjugated D–A terpolymers and their applications in OFETs and OSCs. We will introduce these results in the following order: (i) conjugated terpolymers and applications in OFETs; (ii) conjugated terpolymers and applications in OSCs; and (iii) conjugated terpolymers and applications in both OFETs and OSCs. These terpolymers can be either 2D1A or 1D2A types (Scheme 1).

CONJUGATED D–A TERPOLYMERS FOR APPLICATIONS IN OFETS

Diketopyrrolopyrrole (DPP) is an electron acceptor that has been widely utilized for the construction of conjugated D–A polymers with various electron donors, such as thiophene and bithiophene for organic semiconductors.[18,27–29] These conjugated D–A polymers have led to a number of p-type and ambipolar semiconducting properties with high charge carrier mobilities. For instance, Liu and co-workers designed and synthesized conjugated DPP-based polymer (DPPTTT) with thienothiophene (TT) as the electron-donating moieties, and OFETs with this polymer displayed high hole mobilities up to 10.5 cm^2 V^{-1} s^{-1}.[28] We recently reported the remarkable

[1]Department of Material and Chemical Engineering, Zhengzhou University of Light Industry, Zhengzhou, China and [2]Beijing National Laboratory for Molecular Sciences, CAS Key Laboratory of Organic Solids, Institute of Chemistry, Chinese Academy of Sciences, Beijing, China
Correspondence: Dr Z Liu or Professor D Zhang, Beijing National Laboratory for Molecular Sciences, CAS Key Laboratory of Organic Solids, Institute of Chemistry, Chinese Academy of Sciences, Beijing 100190, China.
E-mail: zitong_@iccas.ac.cn or dqzhang@iccas.ac.cn
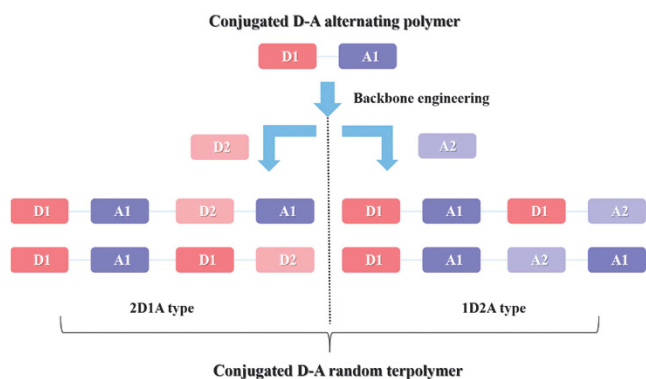
Scheme 1 General structure of conjugated D–A random terpolymers.

enhancement of hole mobility for conjugated DPPTTT upon incorporation of small amounts of tetramethylammonium in the thin film.[18]

A series of DPP-containing terpolymers with two different electron donors have been reported recently. Scheme 2 shows a few of these terpolymers, and the HOMO/LUMO levels and charge mobilities of their thin films are listed in Table 1. Terpolymers P1a–P1g contain TT and selenophene-vinylene-selenophene (SVS) at different molar ratios.[30] In comparison with those of P1f with only SVS and P1g with only TT, the HOMO/LUMO levels of terpolymers P1a–P1e with both SVS and TT at different ratios are slightly varied (Table 1). The hole mobilities of thin films of P1a–P1e increase by enhancing the ratios of SVS in the conjugated backbones, but they are lower than

that of P1f. This may be attributed to the random arrangement of SVS and TT in the conjugated backbone, which is not beneficial for the orderly packing of polymer chains. However, the incorporation of both SVS and TT in P1a–P1e endows them with good solubilities in non-chlorinated solvents (toluene, xylene and tetralin), whereas P1f and P1g are only soluble in chlorinated solvents (for example, $CHCl_3$) and in high-boiling-point solvents. It is known that processing with non-chlorinated solvents is favorable for practical applications of organic semiconductors. In particular, thin films of terpolymers P1c, P1d and P1e processed with non-chlorinated solvents can display hole mobilities higher than $5 \, cm^2 \, V^{-1} \, s^{-1}$. This also holds true for terpolymers P2a–P2c entailing 2,2′-bithieno[3,2-*b*]thiophene and SVS in the backbones at different molar ratios[31] (Scheme 2). P2a and P2b exhibit good solubilities in both chlorinated and non-chlorinated solvents. In comparison, P2e with 2,2′-bithieno[3,2-*b*]thiophene as the electron donor is insoluble in most common organic solvents, whereas P2d with SVS as the electron donor can be dissolved in chlorinated solvents. On the basis of field-effect transistor (FET) studies, P2a and P2b show lower hole mobilities than P2d. However, they can be solution-processed with environmentally benign solvents such as tetrahydrofuran, toluene, xylene and tetralin. The hole mobilities of P2a can reach 6.51 and $6.05 \, cm^2 \, V^{-1} \, s^{-1}$, respectively, by using xylene and tetralin as the processing solvents. Thin films of P2b processed with xylene and tetralin show relatively high charge mobilities up to 4.3 and $3.6 \, cm^2 \, V^{-1} \, s^{-1}$, respectively.

By using a similar strategy, a large and planar conjugated unit was successfully incorporated into conjugated polymers to enhance interchain interactions and hence charge mobilities. We, along with Ajayaghosh *et al.*[32], introduced benzothieno[3,2-*b*]benzothiophene
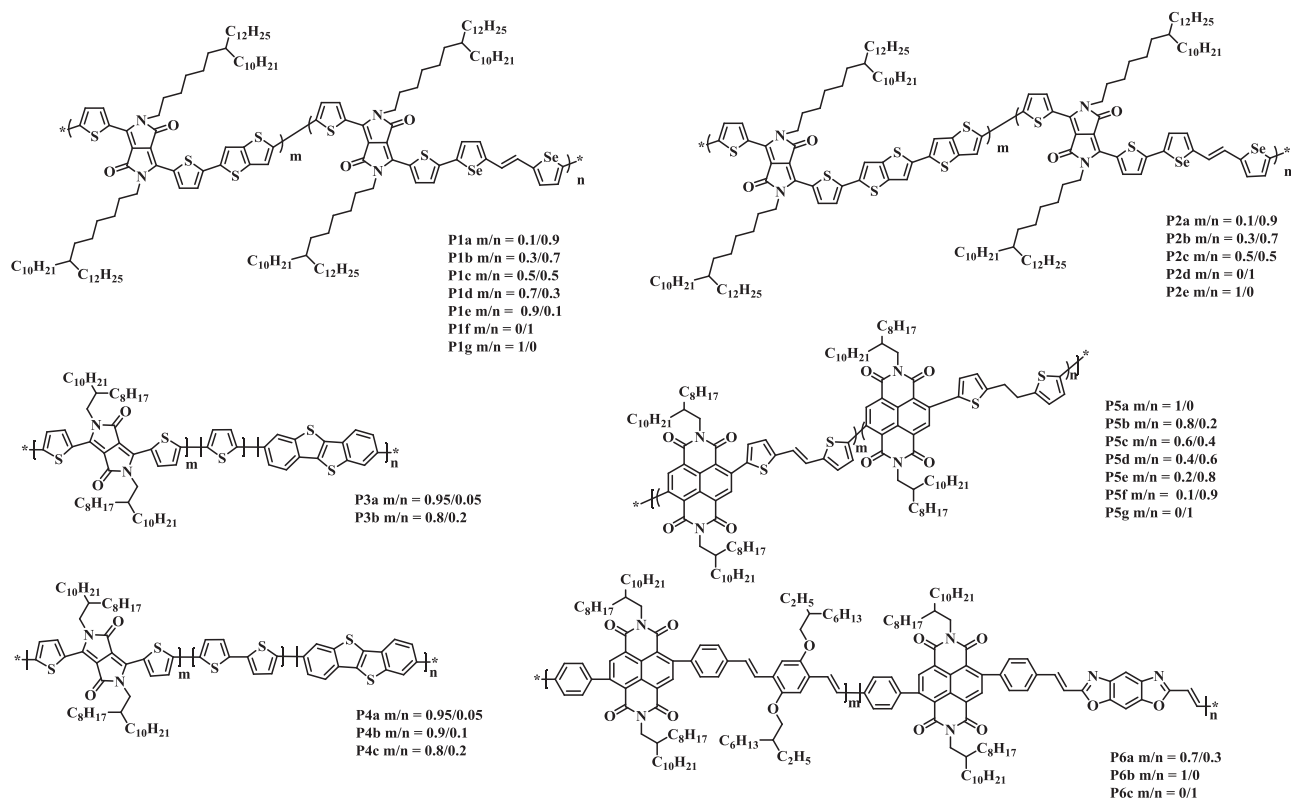

Scheme 2 Chemical structures of conjugated D–A random terpolymers and alternating D–A polymers for organic field-effect transistors.

Table 1 HOMO/LUMO energies of the terpolymers and the respective OFET device data

	HOMO/LUMO (eV)	μ_h^{max} (cm^2 V^{-1} s^{-1})	μ_e^{max} (cm^2 V^{-1} s^{-1})	Device structure	References
P1a	−5.28/−3.99	~4.7[a]	—	BGTC[b]	[30]
P1b	−5.31/−3.97	~7[a]	—	BGTC	[30]
P1c	−5.34/−3.94	~7.1[a]	—	BGTC	[30]
P1d	−5.30/−3.95	~8.1[a]	—	BGTC	[30]
P1e	−5.32/−3.98	~8.1[a]	—	BGTC	[30]
P1f	−5.27/−3.82	~9[a]	—	BGTC	[30]
P1g	−5.36/−3.93	~4.7[a]	—	BGTC	[30]
P2a	−5.49/−3.82	6.51	—	BGTC	[31]
P2b	−5.70/−3.95	4.3	—	BGTC	[31]
P2c	—	—	—	—	[31]
P2d	−5.27/−3.80	>10	—	BGTC	[31]
P2e	—	—	—	—	[31]
P3a	−5.17/−3.79	0.35	—	BGBC[c]	[32]
P3b	−5.16/−3.80	1.47	—	BGBC	[32]
P4a	−5.22/−3.74	1.04	—	BGBC	[32]
P4b	−5.09/−3.76	1.64	—	BGBC	[32]
P4c	−5.08/−3.79	2.47	—	BGBC	[32]
P5a	−5.41/−4.00	0.234	0.99	BGTC	[35]
P5b	−5.36/−3.94	0.1012	0.89	BGTC	[35]
P5c	−5.37/−3.94	0.01091	0.46	BGTC	[35]
P5d	−5.39/−3.92	0.00198	0.314	BGTC	[35]
P5e	−5.40/−3.91	0.00044	0.092	BGTC	[35]
P5f	−5.47/−3.90	0.00000335	0.067	BGTC	[35]
P5g	−5.97/−3.89	—	0.007	BGTC	[35]
P6a	−5.81/−3.94	—	0.0009[b]	BGTC	[36]
P6b	−5.44/−3.75	0.0021[d]	0.00309[b]	BGTC	[36]
P6c	−6.01/−3.98	—	—	BGTC	[36]

Abbreviations: HOMO/LUMO, highest occupied molecular orbital/lowest unoccupied molecular orbital; OFET, organic field-effect transistor.
[a]Estimated with Figure 3a of ref. 30.
[b]Bottom-gate top-contact device architecture.
[c]Bottom-gate bottom-contact device architecture.
[d]Average mobility.

(BTBT) into DPP-thiophene and DPP-bithiophene polymers. BTBT and its derivatives are typical small organic semiconductors with high charge mobilities.[33] However, only few conjugated polymers based on BTBT were reported due to the limited solubility of BTBT, and the polymer with BTBT showed no OFET characteristics owing to a highly twisted backbone.[34] Terpolymers P3a–P3b and P4a–P4c can be dissolved in *o*-dichlorobenzene. By increasing the molar ratio of BTBT unit in the backbones of terpolymers, the interchain packing order degree is slightly enhanced on the basis of grazing incidence X-ray diffraction data; consequently, the charge carrier mobilities of P4c are higher than that of P4a and P4b. Among the terpolymers, P4c shows a relatively high mobility up to 2.47 cm^2 V^{-1} s^{-1}.

Conjugated D–A polymers entailing naphthalene diimide (NDI) as an electron acceptor have also been intensively investigated, and some of these polymers exhibit relatively high electron mobilities. Similarly, two types of electron donors were incorporated into the conjugated backbones to generate terpolymers based on NDI. P5b–P5f and P6a are typical terpolymers with NDI units (Scheme 2). The introduction of non-conjugated dithienylethane units into terpolymers P5b–P5f[35] led to a slight enhancement of LUMO levels, as listed in Table 1. Moreover, by varying the ratio between dithienylvinylene and dithie-nylethane, the morphological, thermal and charge transport properties were successfully modulated for terpolymers P5b–P5f. More importantly, the charge-transporting property was changed from ambipolar to unipolar by gradually increasing the ratio of nonconjugation units

in the backbones of P5a–P5g (Table 1). The conjugated polymer P6b with alternating NDI and *p*-phenylenevinylene moieties exhibits ambipolar semiconducting behavior with average hole and electron mobilities of 0.0021 and 0.00309 cm^2 V^{-1} s^{-1}, respectively.[36] However, the terpolymer P6b afforded by replacing partial *p*-phenylenevi-nylene moieties with benzobisoxazole moieties shows dominant *n*-type semiconducting behavior with electron mobility of 0.0009 cm^2 V^{-1} s^{-1}.

Apart from 2D1A terpolymers, 1D2A terpolymers have also been investigated as semiconducting materials (see below). These studies demonstrate that the incorporation of additional electron donors or acceptors in the conjugated backbones can finely tune the HOMO/LUMO levels, solubilities in organic solvents, interchain packing and charge-transporting properties. In particular, some 2D1A terpolymers can be dissolved in non-chlorinated solvents with relatively high charge mobilities.[30,31]

CONJUGATED D–A TERPOLYMERS FOR APPLICATIONS IN OSCS

As discussed above, the HOMO/LUMO levels and optical gaps as well as interchain packing and thin-film morphology can be finely tuned for conjugated D–A terpolymers by the incorporation of additional electron donors or acceptors in the conjugated backbones. By simply varying the molar ratios of electron donors or acceptors in the backbones, it is possible to widen the absorptions, adjust the HOMO/
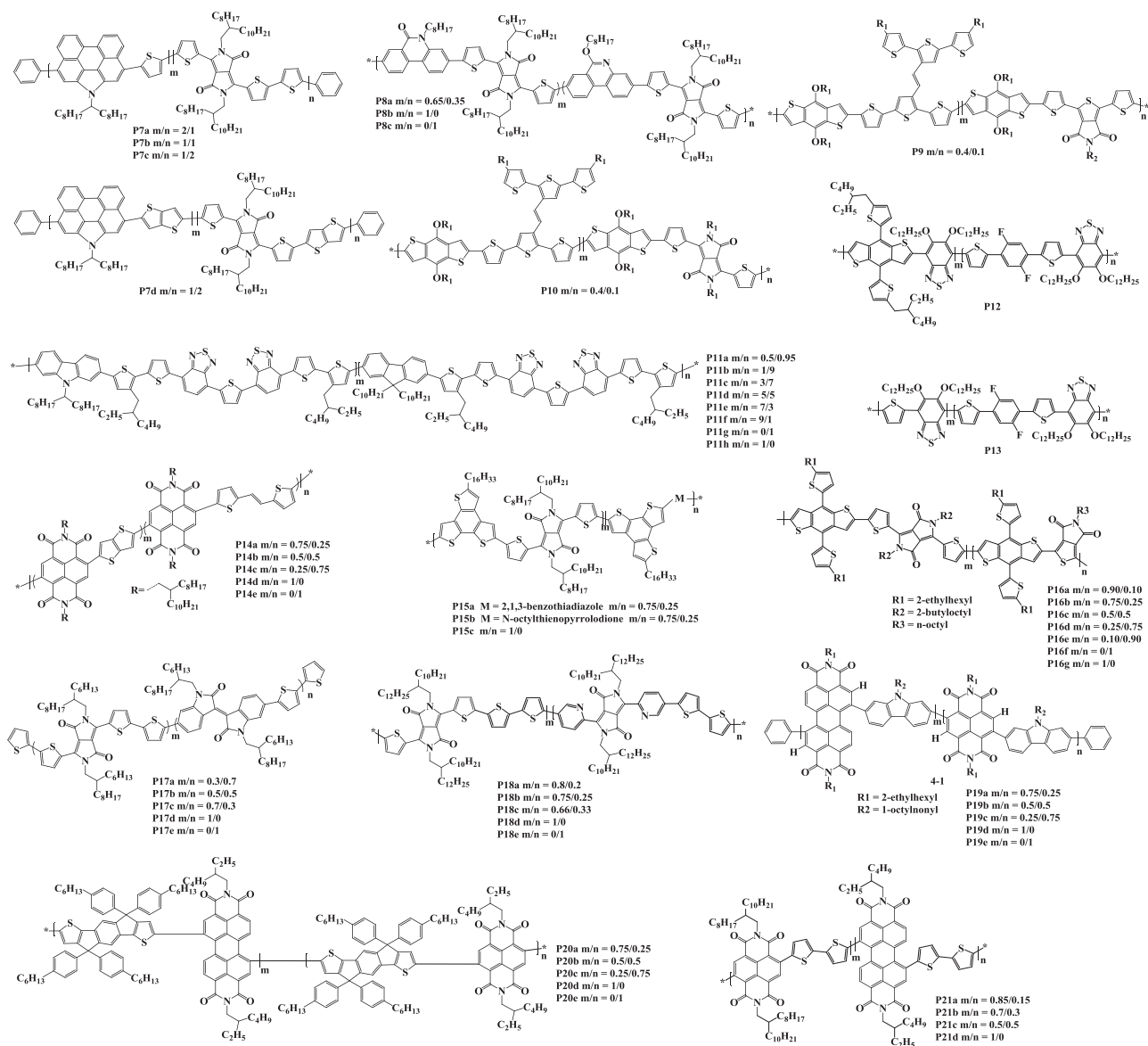
Scheme 3 Chemical structures of terpolymers and compared D–A alternating polymers for organic solar cells.

LUMO levels and improve thin-film morphology, leading to the enhancement of short circuit current (J_{SC}), open circuit voltage (V_{OC}) and fill factor for OSCs. Accordingly, conjugated D–A terpolymers have been intensively investigated as photovoltaic materials for applications in OSCs. Scheme 3 shows representative 2D1A and 1D2A types of conjugated D–A terpolymers for OSCs, and the respective photovoltaic performance data are collected in Table 2. It is known that electron donors and acceptors within photoactive layers of bulk-heterojunction solar cells need to form suitable phase separation structure with optimal domain size to achieve the efficient carrier transport and charge dissociation. Accordingly, PCEs of bulk-heterojunction solar cells are not only affected by HOMO/LUMO levels of electron donors and acceptors but also influenced by thin-film morphologies and crystallinity, as well as phase separation at nanoscale.[4,7] Therefore, it is still hard to establish the correlation between the molecular/solid-state structures of electron donors and acceptors and photovoltaic performances.

2D1A-TYPE CONJUGATED D–A TERPOLYMERS

DPP-based terpolymers P7a-P7c contain both thiophene and 6H-phenanthro[1;10,9,8-cdefg]carbazole (PC) as electron donors at different ratios, whereas both thieno[3,2-b]thiophene and PC in 2:1 ratio are incorporated in the backbone of P7d.[37] Terpolymers P7a–P7d show broad and strong absorptions, and moreover, the HOMO/ LUMO energy levels can be adjusted by varying the molar ratio of the respective two donors. However, the PCEs for the respective solar cells with the terpolymers/PC$_{61}$BM blends are in the range of 0.7–2.8%. Leclerc and co-workers reported DPP-based terpolymer P8a with two weak donors, 6-(octyloxy)phenanthridine and 5-octylphenanthridin-6 (5H)-one at a ratio of 0.35:0.65.[38] They also prepared the respective alternating polymers P8b and P8c. The bulk-heterojunction solar cells with the P8a/PC$_{61}$BM blend exhibit higher fill factor (65%) and PCE (5.62%) than those with P8b/PC$_{61}$BM and P8c/PC$_{61}$BM blends. Furthermore, a high PCE of 6.71% can be achieved for P8a after blending with PC$_{71}$BM. The high photovoltaic performance of P8a is

Table 2 HOMO/LUMO energies of terpolymers and respective OSC device data

	HOMO/LUMO (eV)	Donor or acceptor	V_{OC}	J_{SC}	FF (%)	PCE^{max}	Device structure	References
P7a	−5.38/−3.66	$PC_{61}BM$	0.823	4.07	35.3	1.2	Standard	[37]
P7b	−5.34/−3.69	$PC_{61}BM$	0.748	3.02	28.9	0.7	Standard	[37]
P7c	−5.31/−3.70	$PC_{61}BM$	0.763	6.46	57.8	2.8	Standard	[37]
P7d	−5.29/−3.67	$PC_{61}BM$	0.748	7.78	40.5	2.4	Standard	[37]
P8a	−5.43/−3.92	$PC_{71}BM$	0.85	11.72	67	6.71	Inverted	[38]
P8b	−5.46/−3.95	$PC_{61}BM$	0.86	8.34	51	3.66	Inverted	[38]
P8c	−5.48/−3.93	$PC_{61}BM$	0.82	5.23	58	3.94	Inverted	[38]
P9	−5.04/−3.13	$PC_{61}BM$	0.74	11.65	57.63	5.01	Standard	[39]
P10	−4.99/−3.43	$PC_{61}BM$	0.72	9.96	59.5	4.39	Standard	[39]
P11a	−5.57/−3.91	$PC_{71}BM$	0.79	13.6	58	6.2	Standard	[40]
P11b	−5.56/−3.89	$PC_{71}BM$	0.79	13.5	63	6.7	Standard	[40]
P11c	−5.56/−3.89	$PC_{71}BM$	0.79	12.2	58	5.6	Standard	[40]
P11d	−5.55/−3.85	$PC_{71}BM$	0.78	11.8	60	5.6	Standard	[40]
P11e	−5.52/−3.85	$PC_{71}BM$	0.75	12.1	56	5.1	Standard	[40]
P11f	−5.50/−3.84	$PC_{71}BM$	0.71	12.4	55	4.9	Standard	[40]
P11g	−5.47/−3.79	$PC_{71}BM$	0.76	13.3	58	6.0	Standard	[40]
P11h	−5.62/−3.95	$PC_{71}BM$	0.80	11.2	58	5.2	Standard	[40]
P12	−5.48/−3.65	$PC_{71}BM$	0.83	10.54	67.85	5.95	Standard	[41]
P13	−5.53/−3.72	$PC_{71}BM$	0.86	13.15	68.35	7.71	Standard	[41]
P13	−5.53/−3.72	$PC_{71}BM$	0.86	13.90	70.21	8.50	Inverted	[41]
P14a	−5.54/−3.92	PTB7-Th	0.805	9.60	45.1	3.48	Standard	[42]
P14b	−5.50/−3.92	PTB7-Th	0.790	12.66	48.6	4.86	Standard	[42]
P14c	−5.42/−3.90	PTB7-Th	0.794	13.75	48.3	5.27	Standard	[42]
P14d	−5.59/−3.94	PTB7-Th	0.570	3.56	39.1	0.79	Standard	[42]
P14e	−5.34/−3.88	PTB7-Th	0.795	7.41	49.9	2.94	Standard	[42]
P15a	−5.2/−3.8	$PC_{71}BM$	0.68	10.95	69	5.14	Standard	[43]
P15b	−5.3/−3.9	$PC_{71}BM$	0.72	8.87	66	4.23	Standard	[43]
P15c	−5.2/−3.8	$PC_{71}BM$	0.71	6.30	60	2.68	Standard	[43]
P16a	−5.33/−3.52	$PC_{71}BM$	0.74	10.95	61	4.91	Standard	[44]
P16b	−5.35/−3.51	$PC_{71}BM$	0.76	16.32	51	6.33	Standard	[44]
P16c	−5.42/−3.49	$PC_{71}BM$	0.76	12.95	53	5.26	Standard	[44]
P16d	−5.47/−3.49	$PC_{61}BM$	0.79	7.61	50	3.02	Standard	[44]
P16e	−5.48/−3.49	$PC_{61}BM$	0.82	6.09	42	2.09	Standard	[44]
P16f	−5.49/−3.47	$PC_{61}BM$	0.97	9.25	57	5.10	Standard	[44]
P16g	−5.32/−3.52	$PC_{71}BM$	0.73	12.20	57	5.03	Standard	[44]
P17a	−5.50/−3.79	$PC_{71}BM$	0.48	7.84	57	3.49	Standard	[45]
P17b	−5.62/−3.89	$PC_{71}BM$	0.77	13.52	58	6.04	Standard	[45]
P17c	−5.63/−3.92	$PC_{71}BM$	0.69	12.35	57	4.86	Standard	[45]
P17d	−5.35/−3.81	$PC_{71}BM$	0.63	11.67	63	4.56	Standard	[45]
P17e	−5.65/−3.82	$PC_{71}BM$	0.81	7.06	60	3.43	Standard	[45]
P18a	−5.24/−3.89	$PC_{71}BM$	0.67	15.91	70	6.70	Standard	[46]
P18b	−5.30/−3.93	$PC_{71}BM$	0.69	16.44	71	8.11	Standard	[46]
P18c	−5.32/−3.92	$PC_{71}BM$	0.72	13.51	64	6.29	Standard	[46]
P18d	−5.20/−3.88	$PC_{71}BM$	0.63	15.05	70	6.70	Standard	[46]
P18e	−5.63/−4.03	$PC_{71}BM$	0.83	8.38	59	4.14	Standard	[46]
P19a	−5.67/−3.87	PBDTTT-C	0.78	1.12	28.53	0.25	Standard	[48]
P19b	−5.65/−3.85	PBDTTT-C	0.82	1.11	26.45	0.24	Standard	[48]
P19c	−5.68/−3.86	PBDTTT-C	0.82	0.88	27.97	0.20	Standard	[48]
P19d	−5.65/−3.88	PBDTTT-C	0.84	2.19	30.74	0.57	Standard	[48]
P19e	−5.72/−3.85	PBDTTT-C	0.88	0.98	27.41	0.24	Standard	[48]
P20a	−5.63/−3.86	P3HT	0.63	2.90	60.3	1.11	Standard	[49]
P20b	−5.61/−3.81	P3HT	0.65	3.29	61.4	1.32	Standard	[49]
P20c	−5.65/−3.77	P3HT	0.68	3.62	62.4	1.54	Standard	[49]
P20d	−5.64/−3.90	P3HT	0.62	3.40	65.4	1.38	Standard	[49]
P20e	−5.57/−3.80	P3HT	0.70	2.87	55.3	1.12	Standard	[49]
P21a	−5.49/−3.94	PTB7-Th	0.79	10.71	49.7	4.22	Inverted	[50]
P21b	−5.51/−3.94	PTB7-Th	0.79	11.43	55.4	5.03	Inverted	[50]
P21c	−5.60/−4.00	PTB7-Th	0.79	10.16	41.2	3.33	Inverted	[50]
P21d	−5.42/−3.90	PTB7-Th	0.79	9.05	41.3	2.97	Inverted	[50]

Abbreviations: FF, fill factor; HOMO/LUMO, highest occupied molecular orbital/lowest unoccupied molecular orbital; OSC, organic solar cell; PCE, power conversion efficiency.
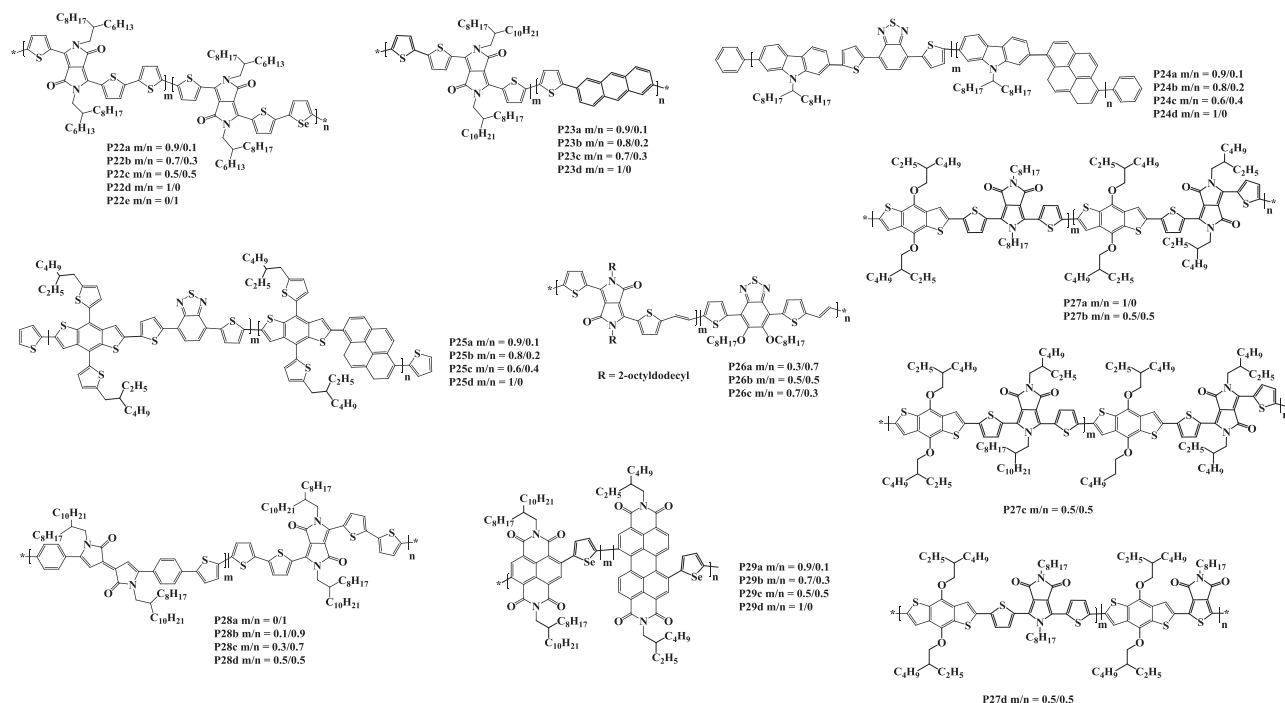
Scheme 4 Chemical structures of terpolymers and compared D–A alternating polymers for both organic field-effect transistors and organic solar cells.

attributed to the fact that the P8a/PC$_{61}$BM and P8a/PC$_{71}$BM blends possess more efficient percolation pathways than the blends of P8b and P8c with either PC$_{61}$BM or PC$_{71}$BM, and accordingly, a higher fill factor results for the blends of P8a with either PC$_{61}$BM or PC$_{71}$BM.

Terpolymers entailing thieno[3,4-*c*]pyrrole-4,6-dione (TPD) were also examined as photovoltaic donors. The terpolymer P9 contains benzo[1,2-*b*:4,5-*b*′]dithiophene (BDT) and terthiophene-vinylene in the backbone. The solar cell with P9/PC$_{61}$BM blend exhibits higher PCE up to 5.01% than with the blend of PC$_{61}$BM and P10, which contains DPP units in the backbone.[39]

Terpolymers P11a–P11f are composed of benzo[*c*][1,2,5]thiadia-zole-thiophene as electron acceptor moieties and fluorene/carbazole as co-donors at different ratios.[40] By tailoring the ratio between fluorene and carbazole, the HOMO and LUMO energy levels of P11a–P11f can be tuned from −5.62 to −5.47 eV and from −3.79 to −3.95 eV, respectively. Grazing-incidence wide-angle X-ray scattering data reveal that the packing order degree of the polymer chains is also strongly affected by varying the ratio between the fluorene and carbazole units in the polymer backbones. The photovoltaic cells with the P11a/PC$_{71}$BM and P11b/PC$_{71}$BM blends exhibit PCEs up to 6.2% and 6.7%, respectively, which are higher than those with the respective blends of P11g and P11h, which are typical alternating D–A polymers with benzo[*c*][1,2,5]thiadiazole-thiophene as electron acceptor moi-eties and fluorene or carbazole as the respective donors. However, the blends of P11c–P11f with PC$_{71}$BM display low photovoltaic perfor-mance. Terpolymers P12 and P13 contain dialkoxybenzothiadiazole as electron acceptor moieties with two different electron donors in the backbones (Scheme 3).[41] The S···F or S···O interactions make the polymeric backbones more planar, and hence the interchain interac-tions are enhanced. The photovoltaic cells with P12/PC$_{71}$BM and P13/PC$_{71}$BM blends exhibit high PCEs up to 5.95% and 7.71%, respectively.[41] Furthermore, after changing the device structure to an inverted one, the PCE with the P13/PC$_{71}$BM blend can be increased to

8.50%, which is among the highest PCE values reported for terpolymers after blending with PC$_{71}$BM.

Apart from being utilized as electron donors for photovoltaic cells, conjugated D–A terpolymers were investigated as electron acceptors for all-polymer solar cells. The NDI-based terpolymers P14a–P14c have TT and dithienylvinylene as co-donors.[42] In comparison with the respective alternating D–A copolymers P14d and P14e, the thin-film electronic absorption and surface roughness can be tuned by varying the TT/dithienylvinylene ratio. The photovoltaic performance of P14a–P14c is higher than that of P14d and P14e after blending with PTB7-Th under the same conditions. The PCE of the PTB7-Th (poly [4,8-bis(5-(2-ethylhexyl)thiophen-2-yl)benzo[1,2-*b*;4,5-*b*′]dithio-phene-2,6-diyl-alt-(4-(2-ethylhexyl)-3-fluorothieno[3,4-*b*] thiophene-)-2-carboxylate-2-6-diyl)])/P14c blend is up to 5.27%.[42]

1D2A-TYPE CONJUGATED D–A TERPOLYMERS

Conjugated D–A terpolymers with one donor moieties and two co-acceptors in the backbones have also been designed and synthesized for photovoltaic studies. Terpolymers P15a and P15b entail benzo[1,2-*b*:3,4-*b*′:5,6-*d*′]trithiophene (BTT) as the donor moieties. DPP and benzothiadiazole are used as co-acceptors for P15a, whereas DPP and N-octylthienopyrrolodione (C8-TPD) are introduced as co-acceptors in the backbone of P15b.[43] Again, the incorporation of additional electron acceptor in the backbone can finely tune the respective HOMO/LUMO levels and electronic absorptions. The P15a/PC$_{71}$BM and P15b/PC$_{71}$BM blends display better photovoltaic performance than the blend of PC$_{71}$BM and P15c, which is an alternating polymer with BTT and DPP, as shown in Table 2.

Terpolymers P16a–P16e contain DPP and TPD as co-electron acceptors and thienyl-substituted benzo[1,2-*b*:4,5-*b*′]dithiophene (BDTT) as electron donor moieties.[44] In comparison with the alternating TPD-BDTT polymer (P16f) and DPP-BDTT polymer (P16g), the incorporation of additional acceptor units in the

Table 3 HOMO/LUMO energies of terpolymers and the respective OSC and OFET device data

	HOMO/LUMO (eV)	Donor or acceptor	V_{OC}	J_{SC}	FF (%)	PCE^{max}	Device structure	$\mu_h{}^{max}$ ($cm^2\,V^{-1}\,s^{-1}$)	$\mu_e{}^{max}$ ($cm^2\,V^{-1}\,s^{-1}$)	Device structure	References
P22a		$PC_{71}BM$	0.67	16.22	67	7.20	Inverted	4.24	2.12	BGTC	[51]
P22b		$PC_{71}BM$	0.67	15.45	67	6.91	Inverted	3.63	2.39	BGTC	[51]
P22c		$PC_{71}BM$	0.66	15.76	65	6.76	Inverted	2.46	2.48	BGTC	[51]
P22d		$PC_{71}BM$	0.68	14.29	70	6.79	Inverted	3.17	2.11	BGTC	[51]
P22e		$PC_{71}BM$	0.65	13.44	64	5.59	Inverted	4.72	5.54	BGTC	[51]
P23a	−5.32/−3.35	$PC_{71}BM$	0.62	13.59	66	5.54	Standard	0.57	—	BGTC	[52]
P23b	−5.28/−3.29	$PC_{71}BM$	0.61	15.50	66	6.24	Standard	0.45	—	BGTC	[52]
P23c	−5.28/−3.22	$PC_{71}BM$	0.56	15.84	51	4.53	Standard	0.37	—	BGTC	[52]
P23d	−5.36/−3.49	$PC_{71}BM$	0.65	7.71	66	3.33	Standard	1.42	—	BGTC	[52]
P24a	−5.56/−3.62	$PC_{71}BM$	0.74	10.60	41	3.22	Standard	0.0001	—	BGBC	[53]
P24b	−5.57/−3.62	$PC_{71}BM$	0.75	9.28	41	2.84	Standard	0.00015	—	BGBC	[53]
P24c	−5.59/−3.64	$PC_{71}BM$	0.78	8.31	43	2.79	Standard	0.0024	—	BGBC	[53]
P24d	−5.52/−3.64	$PC_{71}BM$	0.73	9.54	40	2.82	Standard	0.00006	—	BGBC	[53]
P25a	−5.35/−3.62	$PC_{71}BM$	0.86	10.48	47	4.24	Standard	0.00074	—	BGBC	[53]
P25b	−5.37/−3.67	$PC_{71}BM$	0.87	10.93	53	5.04	Standard	0.0017	—	BGBC	[53]
P25c	−5.38/−3.69	$PC_{71}BM$	0.88	10.30	44	3.98	Standard	0.0038	—	BGBC	[53]
P25d	−5.30/−3.56	$PC_{71}BM$	0.82	8.84	46	3.34	Standard	0.00053	—	BGBC	[53]
P26a	−5.07/−3.20	$PC_{61}BM$	0.60	7.35	58	2.4	Standard	0.05	—	BGTC	[54]
P26b	−5.13/−3.33	$PC_{61}BM$	0.59	3.54	59	1.3	Standard	0.17	—	BGTC	[54]
P26c	−5.16/−3.41	$PC_{61}BM$	0.59	1.52	56	0.5	Standard	0.40	—	BGTC	[54]
P27a	−5.39/−3.28	$PC_{71}BM$	0.90	10.12	72	6.57	Standard	0.00037	—	BGTC	[56]
P27b	−5.25/−3.88	$PC_{71}BM$	0.71	4.43	52	1.64	Standard	0.0003	—	BGTC	[56]
P27c	−5.25/−3.91	$PC_{71}BM$	0.76	5.39	53	2.14	Standard	0.000036	—	BGTC	[56]
P27d	−5.39/−3.48	$PC_{71}BM$	0.87	11.52	70	7.03	Standard	0.00037	—	BGBC	[57]
P28a	−5.15/−3.67	$PC_{71}BM$	0.65	6.09	67	2.67	Standard	0.665	0.197	BGBC	[59]
P28b	−5.18/−3.65	$PC_{71}BM$	0.67	2.52	67	5.12	Standard	0.604	0.219	BGBC	[59]
P28c	−5.20/−3.64	$PC_{71}BM$	0.58	5.11	58	2.14	Standard	0.047	0.016	BGBC	[59]
P28d	−5.24/−3.63	$PC_{71}BM$	0.56	11.84	56	1.07	Standard	0.016	0.003	BGBC	[59]
P29a	−5.54/−3.84	PBDTTT-CT	0.78	6.94	51	2.80	Inverted	—	0.055	BGTC	[60]
P29b	−5.65/−3.89	PBDTTT-CT	0.79	18.55	45	6.29	Inverted	—	0.0071	BGTC	[60]
P29c	−5.65/−3.89	PBDTTT-CT	0.73	9.68	38	2.66	Inverted	—	0.004	BGTC	[60]
P29d	−5.49/−3.84	PBDTTT-CT	0.81	4.16	40	1.36	Inverted	—	0.092	BGTC	[60]

Abbreviations: BGBC, bottom-gate bottom-contact device architecture; BGTC, bottom-gate top-contact device architecture; FF, fill factor; HOMO/LUMO, highest occupied molecular orbital/lowest unoccupied molecular orbital; OFET, organic field-effect transistor; OSC, organic solar cell; PCE, power conversion efficiency.

backbones results in the modulation of the electronic absorptions of the terpolymers. The absorptions of P16a–P16e in the range of 400–650 nm become strong, and their bandgaps increase by increasing the TPD contents in the backbones. However, the bandgaps decrease, and the absorption intensities in the range of 600–900 nm become stronger when more DPP units are incorporated in the backbones for P16a–P16e. Moreover, the HOMO and LUMO energy levels of P16a–P16e are varied from −5.33 to −5.48 eV and from −3.52 to −3.49 eV, respectively, by increasing the molar ratio between TPD and DPP in the backbones of these terpolymers. As expected, the modulation of the electronic absorptions and HOMO/LUMO energy levels can affect the photovoltaic performance of P16a–P16e after blending with $PC_{71}BM$. The PCE of the photovoltaic cell with the P16b/$PC_{71}BM$ blend is up to 6.33%, which is higher than those of the respective blends of P16f and P16g with $PC_{71}BM$.[44]

DPP and isoindigo as electron acceptors show similar electronic absorptions and molecular sizes, and as a result, it is expected that interchain interactions and packing for terpolymers with DPP and isoindigo as co-acceptors such as P17a–P17c would not be largely altered in comparison with the respective alternating D–A polymers P17d and P17e.[45] However, the HOMO level of isoindigo is lower than that of DPP; thus, the incorporation of isoindigo units in the backbones will lower the HOMO levels of terpolymers P17a–17c, leading to a boost of the V_{OC} of the respective photovoltaic cells. The respective blends of P17a–P17c with $PC_{71}BM$ exhibit relatively high photovoltaic performance. For instance, the PCE of the solar cells with the P17b/$PC_{71}BM$ blend is up to 6.04%.[45] Similarly, terpolymers P18a–P18c, which entail dithienyl DPP and pyridine-capped DPP as co-electron acceptors, were designed and investigated.[46] Compared to the corresponding alternating D–A polymers P18d and P18e, terpolymers P18a–18c show remarkably broad absorptions and the HOMO levels are obviously lowered. Furthermore, the grazing-incidence wide-angle X-ray scattering data also reveal that the interchain packing for these terpolymers is beneficial for improving photovoltaic performance. The photovoltaic cell with the P18b/$PC_{71}BM$ blend shows a PCE of 8.11%, which is higher than those with the corresponding blends of P18d and P18e with $PC_{71}BM$.[46] Other DPP-containing terpolymers were also applied for OSCs with PCEs up to 6.8% after blending with $PC_{71}BM$.[47]

In addition, 1D2A-type terpolymers were investigated as electron acceptors for solar cells with high PCEs. Terpolymers P19a–P19c contain perylene diimide (NDI/PDI) as the co-electron acceptors and

carbazole as the donor moieties.[48] However, solar cells with the respective blends of P19a–P19c with PBDTTT-C (poly[(4,8-bis-(2-ethylhexyloxy)-benzo[1,2-*b*;4,5-*b*′]dithiophene)-2,6-diyl-alt-(5,5′-bis (2-thienyl)-4,4,-dinonyl-2,2′-bithiazole)-5′,5″-diyl]) exhibit rather low PCEs. The replacement of carbazole in P19a–P19c with 4,4,9,9-tetrakis (4-hexylphenyl)-indaceno[1,2-*b*:5,6-*b*′]-dithiophene led to terpolymers P20a–P20c.[49] Again, compared to the alternating D–A polymers P20d and P20e, the electronic absorptions and HOMO/LUMO levels of P20a–P20c can be finely tuned by varying the ratio between NDI and PDI. The photovoltaic cell with the P3HT/P20c blend shows a PCE of 1.54%, which is higher than those based on P3HT/P20d (1.38%) and P3HT/P20e blends (1.12%). P21a–P21c are NDI/PDI-based terpolymers with bithiophene as electron donor units.[50] P21a–P21c as electron acceptors after blending with either PTB7 or PTB7-Th show higher photovoltaic performance than the respective blends of P21d with either PTB7 or PTB7-Th. The PCE for the photovoltaic cell with the PTB7-Th/P21b blend as the active layer is up to 5.03%.[50]

The results of both 2D1A and 1D2A types of conjugated terpolymers clearly demonstrate that the incorporation of additional electron donor or acceptor moieties in the backbones is an efficient approach to finely tune the electronic absorptions and HOMO/LUMO levels of conjugated polymers. Although it is still difficult to predict the alteration of interchain packing and thin-film morphology after introducing additional donor or acceptor units, conjugated D–A terpolymers are promising as both electron donors and acceptors for high-performance photovoltaic cells.

CONJUGATED D–A TERPOLYMERS FOR APPLICATIONS IN OFETS AND OSCS

Conjugated D–A random terpolymers for both OFETs and OSCs have rarely been reported. This is simply because the structural requirements for OFETs and OSCs are different. For instance, for OFETs, the polymers need to possess appropriate HOMO or LUMO energy levels, which can match the Fermi energies of the electrodes to facilitate charge injection, whereas for OSCs, the HOMO and LUMO energy levels of conjugated polymers need to be compatible with the respective electron donors or acceptors for efficient charge separation. Conjugated polymers need to absorb strongly in the visible and even in the near-infrared regions for OSCs. Conjugated D–A terpolymers, which have been used in both OFETs and OSCs, are shown in Scheme 4, and the corresponding charge mobilities of OFETs and PCEs of OSCs are listed in Table 3.

2D1A-TYPE CONJUGATED D–A TERPOLYMERS

P22a–P22c are DPP-based terpolymers with selenophene and thiophene as two co-electron donors.[51] On the basis of transfer curves of the respective FETs, the charge carrier mobilities of thin films of P22a–P22c are higher than that of thin film of P22d, which is composed of alternating DPP and thiophene moieties, but terpolymers P22a–P22c exhibit lower charge mobilities than P22e and contain only selenophene as the electron donors. Such charge mobility enhancement is attributed to the improvement of interchain packing order degree for terpolymers containing different amounts of selenophene moieties in their backbones. Terpolymers P22a–P22c were also investigated as electron donors for photovoltaic cells. Among P22a–P22c, P22a displays relatively high photovoltaic performance, with a PCE of 7.2% after blending with PC$_{71}$BM.[51]

Some researchers have reported DPP-based terpolymers P23a–P23c with thiophene and anthracene units as co-electron donors.[52] The incorporation of anthracene units in the backbones of terpolymers will alter the interchain interactions and arrangements. For instance, the

P23b/PC$_{71}$BM blend entails nanofibrils, which are beneficial for charge separation and transport. These terpolymers show relatively high photovoltaic performance, and PCE for the solar cell with the P23b/ PC$_{71}$BM blend can reach 6.24%, which is higher than that with the blend of PC$_{71}$BM with P23d composed of alternating DPP and thiophene units. In comparison, the partial replacement of dithienyl-2′,1′,3′-benzothiadiazole units in P24d with pyrene moieties yields terpolymers P24a–P24c.[53] In a similar way, substitution of partial dithienyl-2′,1′,3′-benzothiadiazole moieties by pyrene units transforms P25d into P25a–P25c.[53] As listed in Table 3, the introduction of more pyrene units in terpolymers P24a–P24c results in the enhancement of charge mobilities in comparison with P24d. This also holds true for P25a–P25c, which show high mobilities in the form of thin films compared to P25d. Furthermore, the HOMO levels of both P24a– P24c and P25a–P25c become low-lying in comparison with those of P24d and P25d, respectively. Accordingly, V_{OC}s of photovoltaic cells with the respective blends of terpolymers and PC$_{71}$BM are enhanced, and PCEs up to 5.04% are yielded[53] (Table 3).

1D2A-TYPE CONJUGATED D–A TERPOLYMERS

DPP and benzothiadiazole as co-electron acceptors are incorporated in the backbones at different ratios in terpolymers P26a–P26c.[54] It is interesting to note that the maximum hole mobilities of P26a–P26c increase from 0.05 to 0.40 cm^2 V^{-1} s^{-1} by increasing the DPP contents in the conjugated backbones. However, PCEs decrease from 2.4 to 0.5% for the blends of P26a–P26c with PC$_{71}$BM as the respective active layers after enhancing the ratio between DPP and benzothiadiazole (Table 3).

A new electron acceptor pyrrolo[3,4-c]pyrrole-1,3-dione (TDPbPDT) was utilized to construct conjugated D–A polymers such as P27a with BDT as electron donor moieties.[55] The incorporation of DPP or TPD acceptor units into P27a affords terpolymers P27b–P27c and P27d, respectively.[56,57] The optical bandgap is reduced from 2.11 eV for P27a to 1.43 and 1.39 eV for P27b and P27c, respectively, by increasing the DPP contents in the conjugated backbones. However, the incorporation of DPP units has a negligible effect on the semiconducting property of these terpolymers; P27b and P27c in the form of thin films show low hole mobilities, similar to P27a. Terpolymers P27b and P27c, after blending with PC$_{71}$BM, show low photovoltaic performance with PCEs of ~ 2% (Table 3). However, the photovoltaic cell with P27d/PC$_{71}$BM blend as the active layer exhibits relatively high PCE up to 7.03%.

Some researchers have recently reported conjugated D–A polymers with bipyrrolylidene-2,2′(1*H*,1′*H*)-dione (BPD).[58] The incorporation of BPD moieties into the backbone of conjugated DPP-thiophene polymer (P28a) affords terpolymers P28b–P28d.[59] The HOMO/ LUMO energy levels and electronic absorptions of P28b–P28d can be modulated by varying the ratios of DPP and BPD. Absorptions in the range of 500–700 nm are enhanced for terpolymers P28b–P28d. The P28b/PC$_{71}$BM blend displays good photovoltaic performance with PCE up to 5.21%, which is higher than that with the P28a/ PC$_{71}$BM blend as the active layer. Moreover, thin film of P28b shows bipolar semiconducting property with hole and electron mobilities up to 0.604 and 0.225 cm^2 V^{-1} s^{-1}, respectively.

Terpolymers P29a–P29c contain PDI and NDI as co-electron acceptors and selenophene as electron donor moieties.[60] Among the terpolymers, P29b shows the best thin-film crystallinity. P29a–P29c were utilized as electron acceptors for all-polymer photovoltaic cells, and the solar cell with the PBDTTT-CT (poly[(4,8-bis[5-(2-ethyl-hexyl)thiophene-2-yl]benzo[1,2-*b*:4,5-*b*′]dithiophene)-2,6-diyl-alt-(4-(2-ethylhexanoyl)-thieno[3,4-*b*]thiophene))-2,6-diyl])/P29b blend as

the active layer shows a PCE of 6.29%,[60] which is much higher than that with the PBDTTT-CT/P29d blend as the active layer. On the basis of FET studies, the electron mobilities of these terpolymers are lowered by increasing the contents of PDI in the backbones as listed in Table 3.

SUMMARY AND OUTLOOK

Conjugated D–A terpolymers with either 2D1A or 1D2A frameworks have been investigated in recent years as high-performance organic semiconductors for FETs and photovoltaic materials for OSCs. With conjugated D–A terpolymers, it is feasible to finely tune the electronic absorptions and HOMO/LUMO energies by varying the ratios of two different donors or two different acceptors. Some terpolymers exhibit relatively high charge mobilities, but most of the terpolymers reported recently display lower charge mobilities than the respective alternating D–A polymers. With regard to applications of conjugated terpolymers in photovoltaic cells, most of the terpolymers after blending with appropriate electron acceptors show relatively good photovoltaic performance, but the PCEs of solar cells with these terpolymers are still under 10%. Conjugated D–A terpolymers that exhibit relatively high charge mobilities and good photovoltaic performance remain limited.

Certainly, conjugated terpolymers deserve further investigations to achieve organic semiconductors with high charge mobilities and photovoltaic materials with high performance. Normally, these terpolymers are prepared by co-coupling of three monomers via Stille or Suzuki coupling reactions. The additional electron donor or acceptor monomers may have different reactivities and solubilities, and accordingly, the terpolymers may possess lower molecular weights than the respective conjugated D–A alternating polymers. Importantly, the random distribution of two electron donors or two acceptors along the conjugated backbones is characteristic for such terpolymers. Such a structural feature will affect the interchain interactions and packing. In addition, this structural characteristic of terpolymers will induce batch-to-batch variations of the samples. Therefore, it is necessary to devise new synthetic approaches to prepare regioregular conjugated D–A terpolymers in which the positions of donor and acceptor moieties in the backbones can be precisely controlled. In fact, recent results clearly indicate that regioregular terpolymers display higher charge mobilities and better photovoltaic performance than the respective random terpolymers.[61–64]

Alternatively, conjugated D–A polymers with more than three types of donor and acceptor moieties can be prepared by coupling more than three monomers in the same way as for terpolymers. The proper combination of electron donors and acceptors in these conjugated polymers will enable us not only to finely modulate the electronic structures of the backbones but also to tune interchain interactions and packing as well as thin-film morphology. In this way, new conjugated polymers with interesting optoelectronic properties are envisaged to be generated by integrating different types of electron donors and acceptors in the conjugated backbones. Quaterpolymers with two types of electron donors and two types of electron acceptors in the conjugated backbones have been recently reported, and applications of these quaterpolymers in photovoltaic cells have yielded PCEs up to 10.3% after blending with PC$_{71}$BM.[65]

On the basis of the consideration that the electronic absorptions and HOMO/LUMO levels can be efficiently tuned for conjugated D–A terpolymers and quaterpolymers, these conjugated polymers are potentially interesting for applications in other optoelectronic devices and even biological areas. For instance, exploration of these conjugated polymers for photoacoustic imaging[66,67] definitely deserves attention.

1 Sirringhaus, H. 25th anniversary article: organic field-effect transistors: the path beyond amorphous silicon. *Adv. Mater.* **26**, 1319–1335 (2014).
2 Lei, T., Pochorovski, I. & Bao, Z. N. Separation of semiconducting carbon nanotubes for flexible and stretchable electronics using polymer removable method. *Acc. Chem. Res.* **50**, 1096–1104 (2017).
3 Lussem, B., Keum, C. M., Kasemann, D., Naab, B., Bao, Z. N. & Leo, K. Doped organic transistors. *Chem. Rev.* **116**, 13714–13751 (2016).
4 Li, Y. F. Molecular design of photovoltaic materials for polymer solar cells: toward suitable electronic energy levels and broad absorption. *Acc. Chem. Res.* **45**, 723–733 (2012).
5 Yao, H. F., Ye, L., Zhang, H., Li, S. S., Zhang, S. Q. & Hou, J. H. Molecular design of benzodithiophene-based organic photovoltaic materials. *Chem. Rev.* **116**, 7397–7457 (2016).
6 Lo, W. Y., Zhang, N., Cai, Z. X., Li, L. W. & Yu, L. P. Beyond molecular wires: design molecular electronic functions based on dipolar effect. *Acc. Chem. Res.* **49**, 1852–1863 (2016).
7 Heeger, A. J. 25th anniversary article: bulk heterojunction solar cells: understanding the mechanism of operation. *Adv. Mater.* **26**, 10–28 (2014).
8 Guo, X. G., Facchetti, A. & Marks, T. J. Imide- and amide-functionalized polymer semiconductors. *Chem. Rev.* **114**, 8943–9021 (2014).
9 Zhao, X. G. & Zhan, X. W. Electron transporting semiconducting polymers in organic electronics. *Chem. Soc. Rev.* **40**, 3728–3743 (2011).
10 Han, A. R., Dutta, G. K., Lee, J. H., Lee, H. R., Lee, S. M., Ahn, H., Shin, T. J., Oh, J. H. & Yang, C. D. Epsilon-branched flexible side chain substituted diketopyrrolopyrrole-containing polymers designed for high hole and electron mobilities. *Adv. Funct. Mater.* **25**, 247–254 (2015).
11 Kang, I., Yun, H. J., Chung, D. S., Kwon, S. K. & Kim, Y. H. Record high hole mobility in polymer semiconductors via side-chain engineering. *J. Am. Chem. Soc.* **135**, 14896–14899 (2013).
12 Kim, G., Kang, S. J., Dutta, G. K., Han, Y. K., Shin, T. J., Noh, Y. Y. & Yang, C. A thienoisoindigo-naphthalene polymer with ultrahigh mobility of 14.4 cm(2)/v.s that substantially exceeds benchmark values for amorphous silicon semiconductors. *J. Am. Chem. Soc.* **136**, 9477–9483 (2014).
13 Sun, B., Hong, W., Yan, Z. Q., Aziz, H. & Li, Y. N. Record high electron mobility of 6.3 cm^{2}V^{-1}s^{-1} achieved for polymer semiconductors using a new building block. *Adv. Mater.* **26**, 2636–2642 (2014).
14 Guo, X., Zhou, N. J., Lou, S. J., Hennek, J. W., Ortiz, R. P., Butler, M. R., Boudreault, P. L. T., Strzalka, J., Morin, P. O., Leclerc, M., Navarrete, J. T. L., Ratner, M. A., Chen, L. X., Chang, R. P. H., Facchetti, A. & Marks, T. J. Bithiopheneimide-dithienosilole/dithienogermole copolymers for efficient solar cells: information from structure-property-device performance correlations and comparison to thieno[3,4-c]pyrrole-4,6-dione analogues. *J. Am. Chem. Soc.* **134**, 18427–18439 (2012).
15 Liu, X. F., Hsu, B. B. Y., Sun, Y. M., Mai, C. K., Heeger, A. J. & Bazan, G. C. High thermal stability solution-processable narrow-band gap molecular semiconductors. *J. Am. Chem. Soc.* **136**, 16144–16147 (2014).
16 Stuart, A. C., Tumbleston, J. R., Zhou, H. X., Li, W. T., Liu, S. B., Ade, H. & You, W. Fluorine substituents reduce charge recombination and drive structure and morphology development in polymer solar cells. *J. Am. Chem. Soc.* **135**, 1806–1815 (2013).
17 Steckler, T. T., Henriksson, P., Mollinger, S., Lundin, A., Salleo, A. & Andersson, M. R. Very low band gap thiadiazoloquinoxaline donor-acceptor polymers as multi-tool conjugated polymers. *J. Am. Chem. Soc.* **136**, 1190–1193 (2014).
18 Luo, H. W., Yu, C. M., Liu, Z. T., Zhang, G. X., Geng, H., Yi, Y. P., Broch, K., Hu, Y. Y., Sadhanala, A., Jiang, L., Qi, P. L., Cai, Z. X., Sirringhaus, H. & Zhang, D. Q. Remarkable enhancement of charge carrier mobility of conjugated polymer field-effect transistors upon incorporating an ionic additive. *Sci. Adv.* **2**, 1600076 (2016).
19 Yao, J. J., Yu, C. M., Liu, Z. T., Luo, H. W., Yang, Y., Zhang, G. X. & Zhang, D. Q. Significant improvement of semiconducting performance of the diketopyrrolopyrrole-quaterthiophene conjugated polymer through side-chain engineering via hydrogen-bonding. *J. Am. Chem. Soc.* **138**, 173–185 (2016).
20 Gao, X. K. & Hu, Y. B. Development of n-type organic semiconductors for thin film transistors: a viewpoint of molecular design. *J. Mater. Chem. C* **2**, 3099–3117 (2014).
21 Yang, J., Wang, H., Chen, J., Huang, J., Jiang, Y., Zhang, J., Shi, L., Sun, Y., Wei, Z., Yu, G., Guo, Y., Wang, S. & Liu, Y. Bis-diketopyrrolopyrrole moiety as a promising building block to enable balanced ambipolar polymers for flexible transistors. *Adv. Mater.* **29**, 1606162 (2017).
22 Luo, H. W. & Liu, Z. T. Recent developments of di-amide/imide-containing small molecular non-fullerene acceptors for organic solar cells. *Chin. Chem. Lett.* **27**, 1283–1292 (2016).

30

23 Zheng, Z., Awartani, O. M., Gautam, B., Liu, D. L., Qin, Y. P., Li, W. N., Bataller, A., Gundogdu, K., Ade, H. & Hou, J. H. Efficient charge transfer and fine-tuned energy level alignment in a thf- processed fullerene- free organic solar cell with 11.3% efficiency. *Adv. Mater.* **29**, 1604241 (2017).

24 Qin, Y. P., Uddin, M. A., Chen, Y., Jang, B., Zhao, K., Zheng, Z., Yu, R. N., Shin, T. J., Woo, H. Y. & Hou, J. H. Highly efficient fullerene-free polymer solar cells fabricated with polythiophene derivative. *Adv. Mater.* **28**, 9416–9422 (2016).

25 Li, S. S., Ye, L., Zhao, W. C., Zhang, S. Q., Mukherjee, S., Ade, H. & Hou, J. H. Energy-level modulation of small-molecule electron acceptors to achieve over 12% efficiency in polymer solar cells. *Adv. Mater.* **28**, 9423–9429 (2016).

26 Zhao, Y., Guo, Y. & Liu, Y. 25th anniversary article: recent advances in n-tyhpe and ambipoar organic field-effect transistors. *Adv. Mater.* **25**, 5372–5391 (2013).

27 Nielsen, C. B., Turbiez, M. & McCulloch, I. Recent advances in the develpment of semiconducting DPP-containing polymers for transistor applications. *Adv. Mater.* **25**, 1859 (2013).

28 Li, J., Zhao, Y., Tan, H. S., Guo, Y. L., Di, C. A., Yu, G., Liu, Y. Q., Lin, M., Lim, S. H., Zhou, Y. H., Su, H. B. & Ong, B. S. A stable solution-processed polymer semiconductor with record high-mobility for printed transistors. *Sci. Rep.* **2**, 754 (2012).

29 Yao, J. J., Cai, Z. X., Liu, Z. T., Yu, C. M., Luo, H. W., Yang, Y., Yang, S. F., Zhang, G. X. & Zhang, D. Q. Tuning the semiconducting behaviors of new alternating dithienyldiketopyrrolopyrrole-azulene conjugated polymers by varying the linking positions of azulene. *Macromolecules* **48**, 2039–2047 (2015).

30 Yun, H. J., Cho, J., Chung, D. S., Kim, Y. H. & Kwon, S. K. Comparative studies on the relations between composition ratio and charge transport of diketopyrrolopyrrole-based random copolymers. *Macromolecules* **47**, 7030–7035 (2014).

31 Yun, H.-J., Lee, G. B., Chung, D. S. & Kim, Y.-H. Novel diketopyrrolopyrrole random copolymers: high charge-carrier mobility from enviromentally benign processing. *Adv. Mater.* **26**, 6612–6616 (2014).

32 Nair, V. S., Sun, J. B., Qi, P. L., Yang, S. F., Liu, Z. T., Zhang, D. Q. & Ajayaghosh, A. Conjugated random donor-acceptor copolymers of [1]benzothieno[3,2-b]benzothiophene and diketopyrrolopyrrole units for high performance polymeric semiconductor applications. *Macromolecules* **49**, 6334–6342 (2016).

33 Takimiya, K., Shinamura, S., Osaka, I. & Miyazaki, E. Thienoacene-based organic semiconductors. *Adv. Mater.* **23**, 4347–4370 (2011).

34 Osaka, I., Abe, T., Shinamura, S., Miyazaki, E. & Takimiya, K. High-mobility semiconducting naphthodithiophene copolymers. *J. Am. Chem. Soc.* **132**, 5000–5001 (2010).

35 Erdmann, T., Fabiano, S., Milian-Medina, B., Hanifi, D., Chen, Z. H., Berggren, M., Gierschner, J., Salleo, A., Kiriy, A., Voit, B. & Facchetti, A. Naphthalenediimide polymers with finely tuned in-chain pi-conjugation: electronic structure, film microstructure, and charge transport properties. *Adv. Mater.* **28**, 9169–9174 (2016).

36 Kolhe, N. B., Ashar, A. Z., Narayan, K. S. & Asha, S. K. Naphthalene diimide copolymers with oligo(*p*-phenylenevinylene) and benzobisoxazole for balanced ambipolar charge transport. *Macromolecules* **47**, 2296–2305 (2014).

37 Deng, Z. Q., Chen, L., Wu, F. & Chen, Y. W. Novel donor – acceptor random copolymers containing phenanthrocarbazole and diketopyrrolopyrrole for organic photovoltaics and the significant molecular geometry effect on their performance. *J. Phys. Chem. C* **118**, 6038–6045 (2014).

38 Guerette, M., Najari, A., Maltais, J., Pouliot, J. R., Dufresne, S., Simoneau, M., Besner, S., Charest, P. & Leclerc, M. New processable phenanthridinone-based polymers for organic solar cell applications. *Adv. Energy Mater.* **6**, 1502094 (2016).

39 Hsiow, C. Y., Wang, H. Y., Lin, Y. H., Raja, R., Rwei, S. P., Chiu, W. Y., Dai, C. A. & Wang, L. Synthesis and characterization of two-dimensional conjugated polymers incorporating electron-deficient moieties for application in organic photovoltaics. *Polymers* **8**, 382 (2016).

40 Kuznetsov, I. E., Akkuratow, A. V., Susarova, D. K., Anokhin, D. V., Moskvin, Y. L., Kluyev, M. V., Peregudov, A. S. & Troshin, P. A. Statistical carbazole-fluorene-TTBTBTT terpolymers as promising electron donor materials for organic solar cells. *Chem. Commun.* **51**, 7562–7564 (2015).

41 Lee, Y. S., Lee, J. Y., Bang, S. M., Lim, B. Y., Lee, J. & Na, S. I. A feasible random copolymer approach for high-efficiency polymeric photovoltaic cells. *J. Mater. Chem. A* **4**, 11439–11445 (2016).

42 Li, X. Z., Sun, P., Wang, Y. L., Shan, H. Q., Xu, J. J., You, C., Xu, Z. X. & Chen, Z. K. Design of three-component randomly incorporated copolymers as non-fullerene acceptors for all-polymer solar cells. *Polym. Chem.* **7**, 2230–2238 (2016).

43 Nielsen, C. B., Ashraf, R. S., Schroeder, B. C., D'Angelo, R., Watkins, S., Song, K., Anthopoulos, T. D. & McCulloch, I. Random benzotrithiophene-based donor–acceptor copolymers for efficient organic photovoltaic devices. *Chem. Commun.* **48**, 5832–5834 (2012).

44 Kang, T. E., Cho, H. H., Kim, H. J., Lee, W., Kang, H. & Kim, B. J. Importance of optimal composition in random terpolymer-based polymer solar cells. *Macromolecules* **46**, 6806–6813 (2013).

45 Jung, J. W., Liu, F., Russell, T. P. & Jo, W. H. Semi-crystalline random conjugated copolymers with panchromatic absorption for highly efficient polymer solar cells. *Energ. Environ. Sci.* **6**, 3301–3307 (2013).

46 Jong, W., Hyungju, A. & Won, H. J. Conjugated random copolymers consisting of pyridine- and thiophene-capped diketopyrrolopyrrole as co-electron accepting units to enhance both jsc and voc of polymer solar cells. *Macromolecules* **48**, 7836–7842 (2015).

47 Jiang, J.-M., Chen, H.-C., Lin, H.-K., Yu, C.-M., Lan, S.-C., Liu, C.-M. & Wei, K.-H. Conjugated random copolymers of benzodithiophene–benzooxadiazole–diketopyrrolopyrrole with full visible light absorption for bulk heterojunction solar cells. *Polym. Chem.* **4**, 5321–5328 (2013)

48 Kozycz, L. M., Gao, D., Tilley, A. J. & Seferos, D. S. One donor-two acceptor (D-A₁)-(D-A₂) random terpolymers containing perylene diimide, naphthalene diimide, and carbazole units. *J. Polym. Sci. Polym. Chem.* **52**, 3337–3345 (2014).

49 Dai, S. X., Cheng, P., Lin, Y. Z., Wang, Y. F., Ma, L. C., Ling, Q. D. & Zhan, X. W. Perylene and naphthalene diimide polymers for all-polymer solar cells: a comparative study of chemical copolymerization and physical blend. *Polym. Chem.* **6**, 5254–5263 (2015).

50 Sharma, S., Kolhe, N. B., Gupta, V., Bharti, V., Sharma, A., Datt, R., Chand, S. & Asha, S. K. Improved all-polymer solar cell performance of n-type naphthalene diimide-bithiophene P(NDI2OD-T2) copolymer by incorporation of perylene diimide as coacceptor. *Macromolecules* **49**, 8113–8125 (2016).

51 Kim, K. H., Park, S., Yu, H., Kang, H., Song, I., Oh, J. H. & Kim, B. J. Determining optimal crystallinity of diketopyrrolopyrrole-based terpolymers for highly efficient polymer solar cells and transistors. *Chem. Mater.* **26**, 6963–6970 (2014).

52 Ju, H. J., Yang, Y., Wang, Z. J., Yang, S. F., Liu, Z. T., Zhang, G. X. & Zhang, D. Q. Conjugated terpolymers synthesized by incorporating anthracene units into the backbones of the diketopyrrolopyrrole-based polymers as electron donors for photovoltaic cells. *Polym. Chem.* **7**, 6798–6804 (2016).

53 Kim, J. H., Kim, H. U., Kang, I. N., Lee, S. K., Moon, S. J., Shin, W. S. & Hwang, D. H. Incorporation of pyrene units to improve hole mobility in conjugated polymers for organic solar cells. *Macromolecules* **45**, 8628–8638 (2012).

54 Li, H., Liu, F. B., Wang, X. D., Gu, C. L., Wang, P. & Fu, H. B. Diketopyrrolopyrrole-thiophene-benzothiadiazole random copolymers: an effective strategy to adjust thin-film crystallinity for transistor and photovoltaic properties. *Macromolecules* **46**, 9211–9219 (2013).

55 Tamilavan, V., Roh, K. H., Agneeswari, R., Lee, D. Y., Cho, S., Jin, Y., Park, S. H. & Hyun, M. H. Pyrrolo 3,4-c pyrrole-1,3-dione-based large band gap polymers containing benzodithiophene derivatives for highly efficient simple structured polymer solar cells. *J. Polym. Sci. Polym. Chem.* **52**, 3564–3574 (2014).

56 Tamilavan, V., Roh, K. H., Agneeswari, R., Lee, D. Y., Cho, S., Jin, Y., Park, S. H. & Hyun, M. H. Benzodithiophene-based broad absorbing random copolymers incorporating weak and strong electron accepting imide and lactam functionalized pyrrolo[3,4-*c*] pyrrole derivatives for polymer solar cells. *Macromol. Chem. Phys.* **216**, 996–1007 (2015).

57 Tamilavan, V., Roh, K. H., Agneeswari, R., Lee, D. Y., Cho, S., Jin, Y., Park, S. H. & Hyun, M. H. Highly efficient imide functionalized pyrrolo[3,4-c]-pyrrole-1,3-dione-based random copolymer containing thieno[3,4-c]pyrrole-4,6-dione and benzodithiophene for simple structured polymer solar cells. *J. Mater. Chem. A* **2**, 20126–20132 (2014).

58 Cai, Z. X., Guo, Y. L., Yang, S. F., Peng, Q., Luo, H. W., Liu, Z. T., Zhang, G. X., Liu, Y. Q. & Zhang, D. Q. New donor-acceptor-donor molecules with pechmann dye as the core moiety for solution-processed good-performance organic field-effect transistors. *Chem. Mater.* **25**, 471–478 (2013).

59 Qi, P. L., Wang, Z. J., Liu, Z. T., Yang, S. F., Yang, Y., Yao, J. J., Zhang, G. X. & Zhang, D. Q. Conjugated donor-acceptor terpolymers entailing the Pechmann dye and dithienyl-diketopyrrolopyrrole as co-electron acceptors: tuning HOMO/LUMO energies and photovoltaic performances. *Polym. Chem.* **7**, 3838–3847 (2016).

60 Hwang, Y. J., Earmme, T., Courtright, B. A. E., Eberle, F. N. & Jenekhe, S. A. n-type semiconducting naphthalene diimide-perylene diimide copolymers: controlling crystallinity, blend morphology, and compatibility toward high-performance all-polymer solar cells. *J. Am. Chem. Soc.* **137**, 4424–4434 (2015).

61 Lee, J. H., Park, G. E., Choi, S., Lee, D. H., Um, H. A., Shin, J., Cho, M. J. & Choi, D. H. Effect of the thiophene and selenophene moiety in regular terpolymers on the performance of thin film transistors and polymer solar cells. *Polymer* **94**, 43–52 (2016).

62 Deng, P., Wu, B., Lei, Y., Cao, H. & Ong, B. S. Regioregular and random difluorobenzothiadiazole electron donor-acceptor polymers semiconductors for thin-film transistors and polymer solar cells. *Macromolecules* **49**, 2541–2548 (2016).

63 Ko, E. Y., Park, G. E., Lee, D. H., Um, H. A., Shin, J., Cho, M. J. & Choi, D. H. Enhanced performance of polymer solar cells comprising diketopyrrolopyrrole-based regular terpolymer bearing two different π-extended donor units. *ACS Appl. Mater. Interfaces* **7**, 28303–28310 (2015).

64 Liu, Y., Li, G., Zhang, Z., Wu, L., Chen, J., Xu, J., Chen, X., Ma, W. & Bo, Z. An efficient way to reduce energy loss and enhance open-circuit voltage in polymer solar cells based on a diketopyrrolopyrrole polymer containing three regular alternating units. *J. Mater. Chem. A* **4**, 13265–13270 (2016).

65 Kang, S. H., Kumari, T., Lee, S. M., Jeong, M. & Yang, C. Densely packed random quarterpolymers containing two donor and two acceptor units: controlling absorption ability and molecular interaction to enable enhanced polymer photovoltaic devices. *Adv. Energy Mater.* **7**, 1700349 (2017).

66 Cui, D., Xie, C. & Pu, K. Development of semiconducting polymer nanoparticles for photoacoustic imaging. *Macromol. Rapid Commun.* **38**, 1700125 (2017).

67 Jiang, Y. & Pu, K. Advanced photoacoustic imaging applications of near-infrared absorbing organic nanoparticles. *Small* **13**, 1700710 (2017).

Hewei Luo received his BSD in Chemistry from Zhengzhou University in 2009 and PhD in Organic Chemistry from ICCAS in 2015. He is a lecturer in School of Materials and Chemical Engineering at Zhengzhou University of Light Industry at present. His research mainly focuses on organic semiconducting materials and lithium ion battery.

Zitong Liu received his BSD in Chemistry from Jilin University in 2003 and PhD in Organic Chemistry from ICCAS in 2008. He is now an associate Professor at the Institute. His research interests include design, synthesis of organic conjugated small molecules/polymers toward optoelectronic materials.

Deqing Zhang received his PhD from Ruprecht-Karls University Heidelberg in 1996 under the supervision of Prof. Dr HA Staab. He is currently a Research Professor at ICCAS. His research interests include development of external stimuli-responsive molecular systems for molecular switches, logic gates and chemo/biosensors. He is also interested in the design and synthesis of organic conjugated molecules toward functional assemblies and materials. He has published more than 300 papers in scientific journals. He serves as an Editorial Advisory Board member of several scientific journals. He is one of the co-editors of *ACS Omega*.